PHYSICS DEPARTMENT

RUTGERS
THE STATE UNIVERSITY
OF NEW JERSEY

Kinetic Theory and Turbulent Discontinuities

Joseph A. Johnson III, Lin I, Yuan Li,
Raghu Ramaiah, Jaime P. Santiago

Kinetic Theory and Turbulent Discontinuities

Joseph A. Johnson III, Lin I, Yuan Li, Raghu Ramaiah, and Jaime P. Santiago

Department of Physics
Rutgers University, New Brunswick, New Jersey 08903

May 15, 1981

Abstract

This document is a final technical report on a National Aeronautics and Space Administration research grant titled "The Physics of Turbulent Flow", NSG 3280, June 1, 1979 to May 31, 1980, from NASA Lewis Research Center. The investigators proposed to use shock tube discontinuities so as to test and extend a kinetic theory of turbulence. In shock wave and contact surface fluctuations, coherent phenomena have been found which provide new support for the microscopic nonempirical approach to turbulent systems, especially those with boundary layer-like instabilities.

Table of Contents

I. Introduction

The need to develop a complete theory of turbulence has become urgent. The current potpourri of empirical data fits, phenomenological models, and computer based simulations are becoming more and more unacceptable due to escalating costs and increasingly inadequate achievements. More importantly, they share a fundamental deficiency: traditional approaches violate form invariance and are ultimately inconsistent with the basic laws of physics.

Recently, by contrast, a kinetic theory of turbulence derived from basic principles and without empirical constants has been developed. In this theory, with the assumption of rigid molecular chaos removed, turbulent effects become an explicit part of the fluid equations; expressions are obtained for familiar quantities such as fluctuations in spontaneous stress and heat flux, Reynold's stress and turbulent heat flux. Other effects such as reaction rate distortion in turbulent flows are predicted. We have therefore sought to test some of these expectations using the boundary layer-like discontinuities in shock tube flow. In this report, we review some of our activities during the year of NASA support and speculate on their implications.

II. Density Measurements form Crossed Beams at High Extinctions

The importance of intersecting beams of radiation as an alternative to hot wire anemometry has already been shown by Fisher and Krause[1]. We wish to extend their analyses so that the technique might be applied to the unstable contact surfaces which we have recently reported[2]. For this, we use a dilute mixture of $N_2O_4 \rightleftarrows 2\ NO_2$ in N_2 strongly absorbing at 4350 Å; other experimental details can be found in reference 2.

Referring to Fig. 1, the beam intersection point has coordinates (x,y,z); ξ, η, and τ define distances from this point in the x,y and z directions. If K is the extinction coefficient for a given species in the turbulent flow, then K is a function of position and time and the statistical fluctuations in K will yield statistical fluctuations in a flow property. For beam S_1D_1, the intensity recorded at D_1 at time t is:

$$I_1(t) = I_o \exp\{ - \int K(x,y + \eta,z, t)\, d\eta\} \quad . \qquad (1)$$

The instantaneous extinction coefficient written as the sum of its time-average mean value and a fluctuation relative to this value is:

$$K(x,y +\eta, z, t) = K_{D.C.} + k(x,y + \eta, z, t) \quad . \qquad (2)$$

Further, determining $\langle I_1 \rangle = I_o \exp(-K_{D.C.})$, eq. (1) becomes $I_1(t) = \langle I_1 \rangle \exp\{-\int k(x,y + \eta, z,t)\, d\eta\}$. With similar treatments for S_2D_2, we obtain:

$$i_1(t) = \frac{I_1}{\langle I_1 \rangle} = e^{-\rho_1};\ i_2(t) = \frac{I_2}{\langle I_2 \rangle} e^{-\rho_2} \quad . \qquad (3)$$

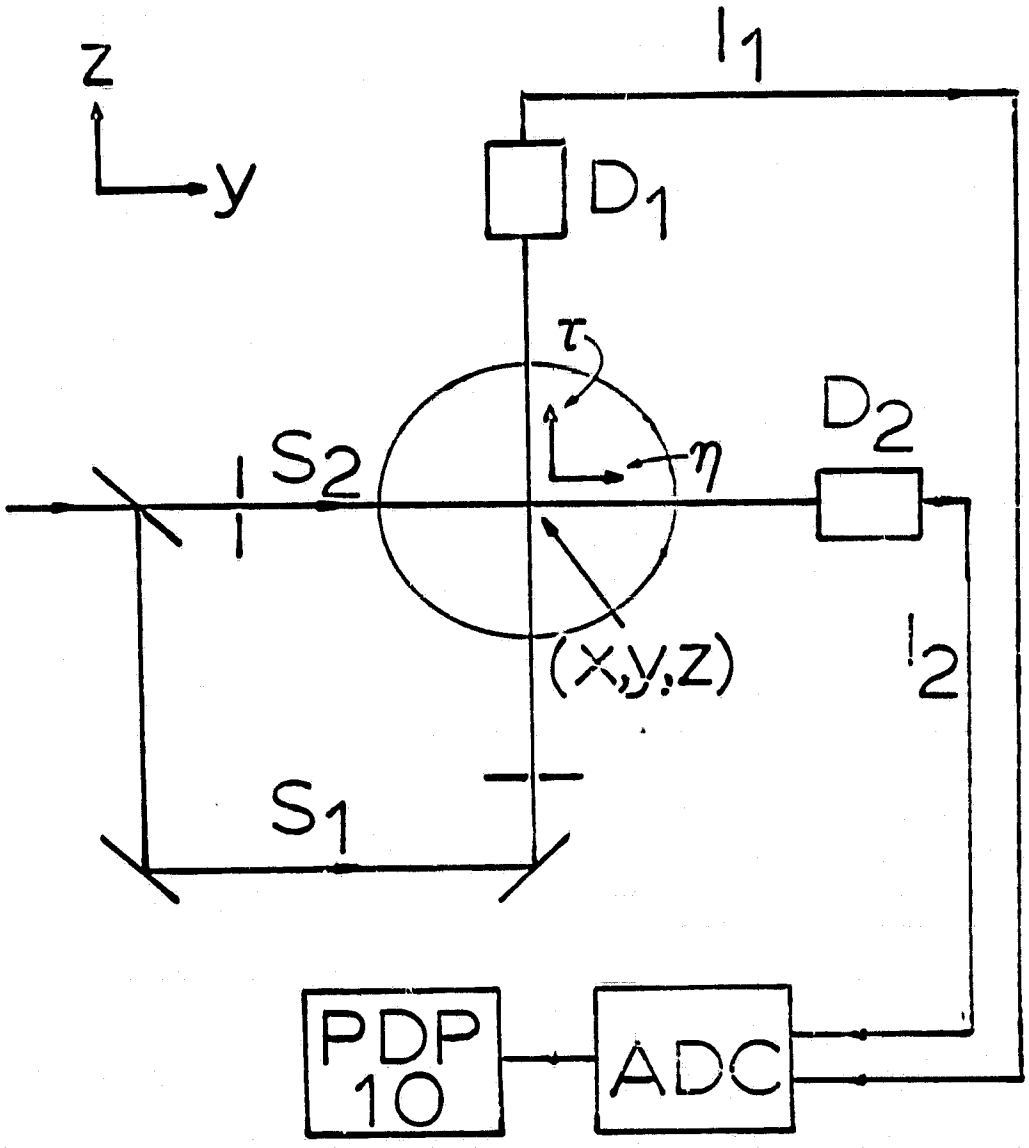

Figure 1. The cross-beam correlation experiment. The circle represents the cross section of our shock tube. The unsteady flow is into the plane of the paper. S_1, S_2, D_1, D_2 are the two sources and detectors of light (λ = 4350 Å) from the Hg-vapour lamp. The output of the photomultiplier tubes (PMT) is fed into the A.D.C. (BIOMATION 8100) and then to the PDP-10 via interface.

Eqs. (3) are the modified detector currents which are fluctuations about a local average level specified by $\langle I_1 \rangle$ and $\langle I_2 \rangle$.

Taking the logarithmic product of eqs. (3) and integrating over T

$$\frac{1}{T}\int_0^T \ell n\, i_1(t) \cdot \ell n\, i_2(t)\, dt = \int d\eta d\tau \{\frac{1}{T}\int_0^T k(n, y+\eta, z, t) \cdot k(x, y, z+\tau, t) dt\}$$

$$= F(x,y,z) \quad . \qquad (4)$$

$F(x,y,z)$ is the covariance of the fluctuations along S_1D_1 and S_2D_2. Assuming a stochastic nature for the fluctuations, the important contributions to $F(x,y,z)$ will come from a correlated area about the beam intersection point. Defining this correlated area as A, we obtain:

$$F(x,y,z) = \frac{1}{T}\int_0^T \ell n i_1(t) \cdot \ell n\, i_2(t) = \overline{k^2(x,y,z)}\, A \quad . \qquad (5)$$

The new relationship above is similar to the one derived in reference 1; however, we have avoided their restricted forms for $i_1(t)$ and $i_2(t)$ which would only apply to weak extinctions. The measured quantity $F(x,y,z)$ is directly proportional to the local turbulent intensity at the point of beam intersection.

Using this approach, the gross features which we observe in the point density fluctuations in the NO_2 driver gas mixtures are the same as those previously reported from pressure, interferometric, and line-averaged absorption measurements[2]. Bursting behavior is clearly indicated in the $\overline{k^2(x,y,z)}$ histories. In addition, power spectra for

the fluctuations all show a dominant mode at about 400 Hz with increasing harmonics at increasing flow velocity. These results are illustrated by the data in Figures 2 and 3. The emergence of a unique "characteristic" frequency for unstable contact surfaces is reminiscent of similar effects in turbulent bursts associated with wall boundary layers and free jets at transition[3,4]. This reinforces the sense of phenomenological kinship between the contact surface and other discontinuities for which the boundary layer approximation seems appropriate[5]. However, the underlying physical significance of these frequencies is not yet determined.

References

1. M.J. Fisher and F.R. Krause, J. Fluid Mech. 28, 705 (1967)
2. J.A. Johnson III, W.R. Jones and J. Santiago, J. Phys. D: Appl. Phys. 13, 1413 (1980)
3. J.H. Strickland and R.L. Simpson, Phys. Fluids 18, 306 (1975)
4. R.A. Antonia, H.Q. Dank and A. Prabhu, Phys. Fluids 19, 1680 (1976)
5. L. Landau and E. Lifshitz, Fluid Mechanics, (Addison-Wesley, Reading, Mass., 1959)

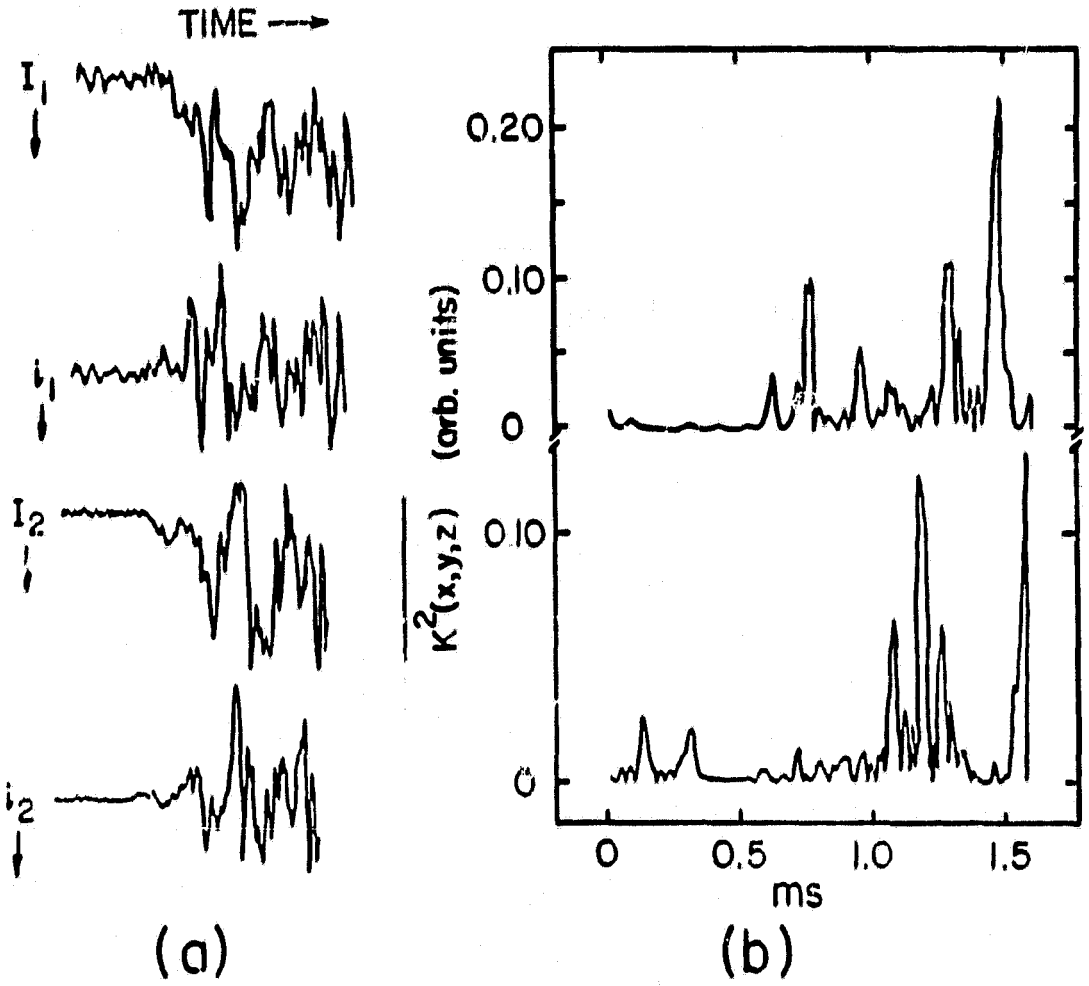

Figure 2. Crossed Beam Data from the Turbulent Contact Surface. (a) Samples of Input Data. The first and third traces are the absorption of beams S_1D_1 and S_2D_2 at 4350 Å. The arrival of the contact surface with NO_2 occurs about 450 μs after the display trigger signal. The second and fourth traces are the absorption at S_1D_1 and S_2D_2 normalized to the secular trends in the first and third traces respectively. Firing conditions were[2]: the driver gas mixture was 2% $N_2O_4 \pm 2NO_2$ in N_2 at room conditions; the driven gas was N_2; the shock wave Mach number, M_s, was $M_s = 1.6$; and the gas velocity at the contact surface was $U_2 = 313$ m/s. The signals shown are 1240 μs long in laboratory time; the vertical scales are arbitrary (linear) units. (b) Samples of the Point Density Fluctuations. (See text, equation (5).) The upper trace is the crossed beam covariance for the data in (a). The lower trace is that for a similar firing at $M_s = 3.2$ for which the contact surface arrived at a time roughly coincident with the display trigger.

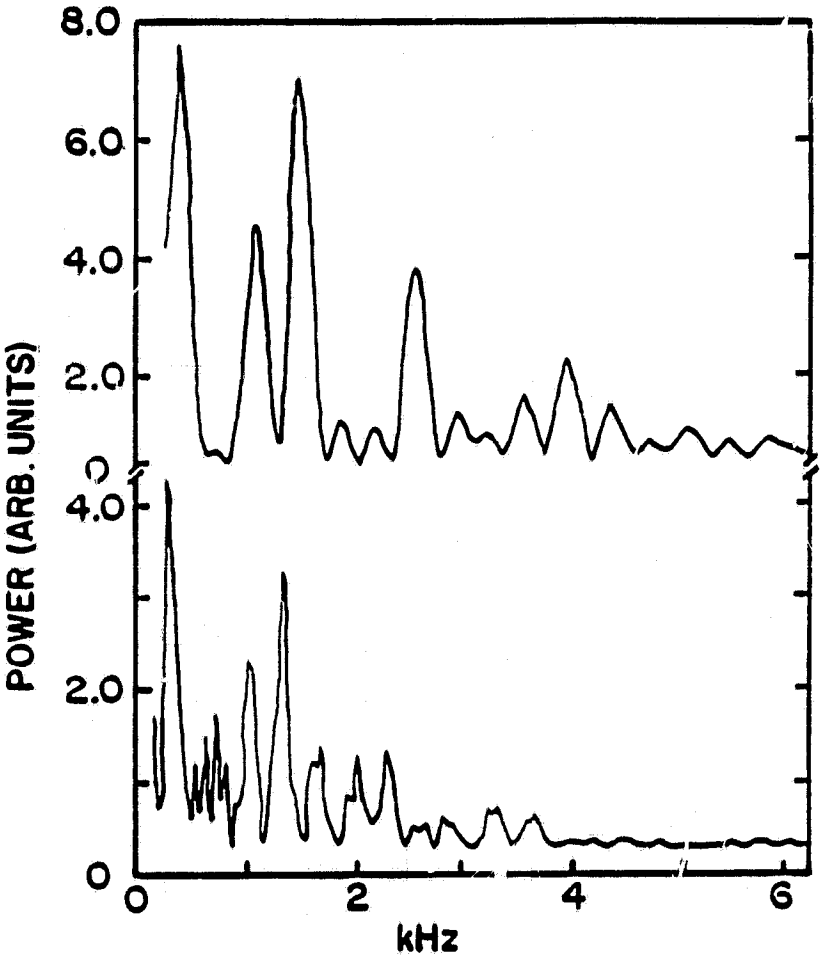

Figure 3. Turbulent Power Spectra at the Contact Surface. The upper and lower traces are from the corresponding data in Figure 2(b).

III. Turbulence in Argon Shock Waves

Gasdynamic discontinuities are known to be inherently unstable when the pressure gradient and the density gradient are opposed[1]. For example, detonation waves show turbulent bursts as a result of the post-ignition expansion of the burning mixture of gases[2]. Contact surfaces provide turbulent intermixing of the otherwise separated gases when a large increase in density associates with a perturbative decrease in pressure at the front[3]. In these examples, the vorticity required for turbulence comes from curvature at the discontinuity[4]. An ionizing collisional discontinuity can also show curvature[5]; a variety of mechanisms can be suggested which might cause the growth[6] and enhanced manifestation[7] of random fluctuations in it. Therefore, we have chosen to look for turbulent effects in ionizing shock waves in argon.

Our shock waves are produced in a cylindrical arc discharge stainless steel shock tube of 5 cm diameter and 185 cm length. The tube is pumped down to less than 10^{-5} Torr before filling. The shock tube is filled with high purity room temperature argon and fired without the use of a diaphragm. No use is made of any external magnetic fields. The discharge is generated by triggering a 14.5 μF capacitor charged to 18.5 kV and typically takes about 50 μsec for completion. The shock wave's speed can be varied between 5×10^5 cm/sec and 3×10^6 cm/sec by varying the initial filling pressure between 250 mTorr and 25 mTorr. The test section is 160 cm from the discharge. Two piezoelectric pressure transducers with 15 cm

separation are positioned fore and aft of the test section's window. At the window, a pair of lenses and a pinhole diaphragm are used to collect white light emission (with a 3.5 mm x 1 mm spatial resolution). At the same location, two steel probes of 0.75 mm diameter are placed in the tube with varying separation along the axis of the tube. The probes are biased at negative voltage so as to collect ion current.

The pressure transducer signals and the white light emission signals are used to determine the velocities of the shock waves which we produce. The white light signals are also used to confirm the general qualitative features of the data from the various probe signals. The probe signals are sent simultaneously to a transient ADC recorder (Biomation 8100) which has a 25 MHz bandwidth in the chopped mode. The digitized data from the probe current are used to obtain the plasma power spectrum via a Fast Fourier Transform. The phases of the Fourier transforms are compared; the wave number, k, is obtained using $\Delta\sigma = i\mathbf{k}\cdot(\Delta\gamma) = ik_z\Delta z$ where $\Delta\sigma$ is the phase difference and Δz is the separation of the two probes.

With these several diagnostics, we have confirmed the existence of turbulent-like fluctuations in collisional shock waves. Figure 1 illustrates this with the probe signals from three different shock tube firings under three different conditions. The arrival of the shock wave is observed as a sharp rise in the probe current. In each case, rapid irregular oscillations in the signals are found which persist for 5 to 25 μsec; they are then followed by a relatively quiet decay

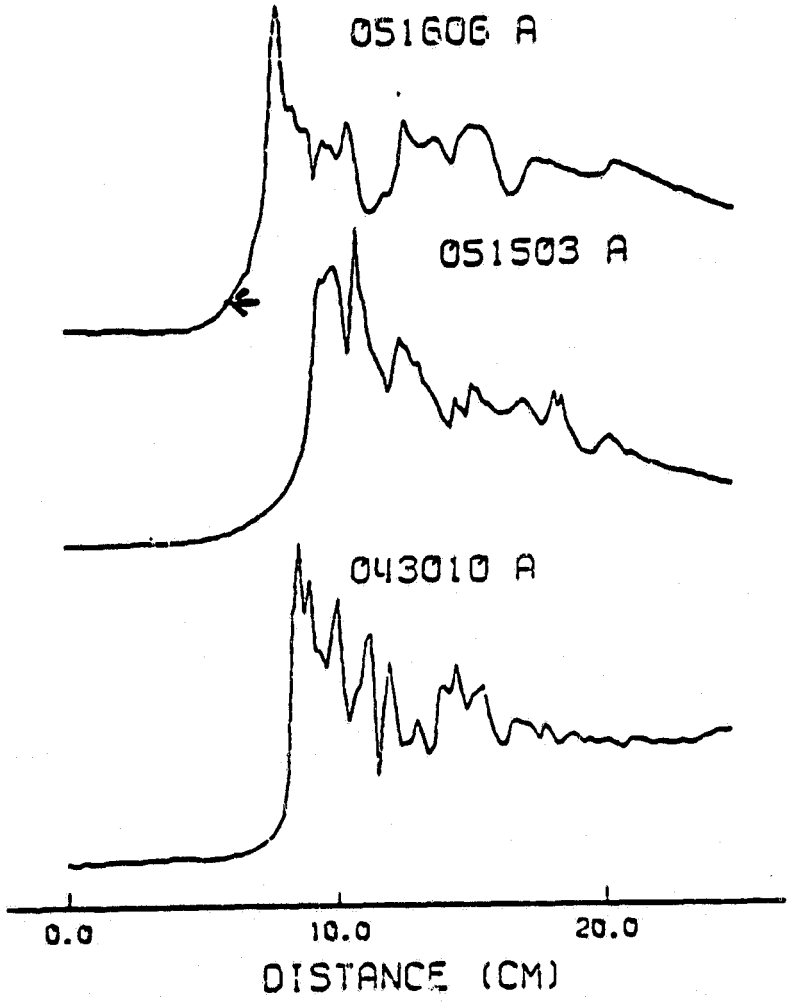

Figure 1. Sample Data: Probe Signals. Top Trace: #051606A, p = 100 mTorr, M = 16. Middle Trace: #051503A, p = 60 mTorr, M = 26. Lower Trace: #043010A, p = 40 mTorr, M = 36. (M is the Mach number of the shock wave and p is the pressure in the shock tube prior to the discharge of the capacitor.) Laboratory time, t_L, and distance, d_s, plotted above are related by $d_s = t_L \times V_g$ where V_g is the flow velocity at the shock front.

phase. The data are shown in a frame of reference fixed with respect to the gas at the shock wave. The general features of the fluctuations appear to be Mach number independent; that is, the fluctuations are essentially frozen in the moving frame, lasting from 12 to 15 cm, with the same overall shape.

Fourier analyses of the fluctuations in probe signals provide further evidence of a frozen pattern. In Figure 2a are shown the power spectra of two probe signals (designated A and B) with probe B 0.75 cm downstream from probe A along the shock tube's axis; the pressure in the shock tube is 30 mTorr and the shock wave is moving at Mach number M = 42 at the test section. The third spectrum, designated B', is obtained from a shock tube firing at p = 40 mTorr and M = 36. The frequencey axis for B' is adjusted by a factor of 1.16 in accordance with the change in Mach number. We notice that there is a general peak to peak correspondence in A and B. This suggests a longitudinal reproducibility in the statistical behaviors of the shock front fluctuations. The spectrum B' suggests that the fluctuations in two different firings under similar conditions are similar in their statistical features. In addition, we find that the phase velocity of each mode is about the same as the group velocity. This is illustrated in Figure 2b for the two firings in Figure 2a; the dispersion relations for A and B and for A' (not shown) and B' are nearly linear. In both cases, the group velocity is slightly lower than the measured velocity of the shock wave ($v_g/v_s \sim 0.9$).

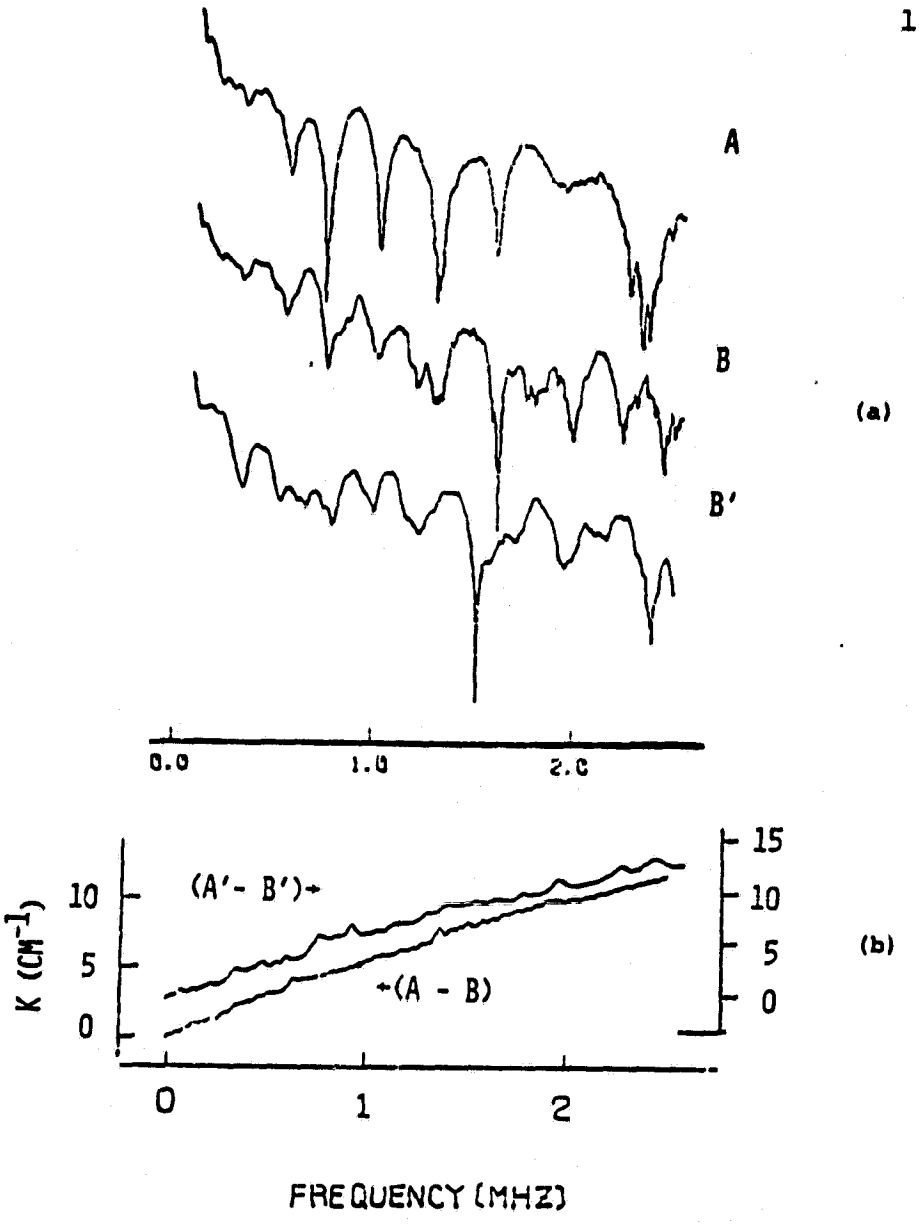

Figure 2. Sample Data: Spectral Analyses. (a) Power Spectra. Upper and middle traces are from two probes (A and B) separated by 0.75 cm along the axis of the shock tube for a firing with p = 30 mTorr and M = 42. The lower trace (B') is from a firing with p = 40 mTorr and M = 36. The vertical scales are in arbitrary (logarithimic) units. The horizontal scale is frequency (MHz). (b) Dispersion Relations. The lower trace is for signals A-B above. The top trace is for signals A'-B' for which B' is shown above.

However, v_g is approximately the same as the local flow speed behind the shock front. Therefore, in the frame moving with the flow velocity, the group velocity is essentially zero,- as required for a frozen fluctuation pattern.

The spatial evolution (in the moving gas frame) of selected modes in the probe signals has been obtained by the inverse descrete Fourier Transform after filtering by a "brickwall" type, zero phase, digital bandpass filter with a variable bandwidth. Samples of these data are shown in Figure 3. We find that the spectra are quantized and that the fundamental mode has a wave length of about 2.5 cm, i.e., about one-half the diameter of the shock tube. All the modes are heavily damped; however, the higher the frequency, the faster the growth and damping rates. Finally, we notice that the envelopes of different modes oscillate with different periods, thereby suggesting the possiblility of intermodal energy transfer.

From these measurements, we see that the fluctuations in our shock waves display typical turbulent signatures. The presence of a dominant mode in the fluctuation spectra which we find is appropriate for turbulence in its earliest phases[8]. The reproducibility of the characterizing modes in the fluctuations which we have shown is to be expected for gas systems where the boundary conditions are unchanged[9]. The use of a point diagnostic provides us evidence for turbulence in a shock front which is more conclusive than that available from

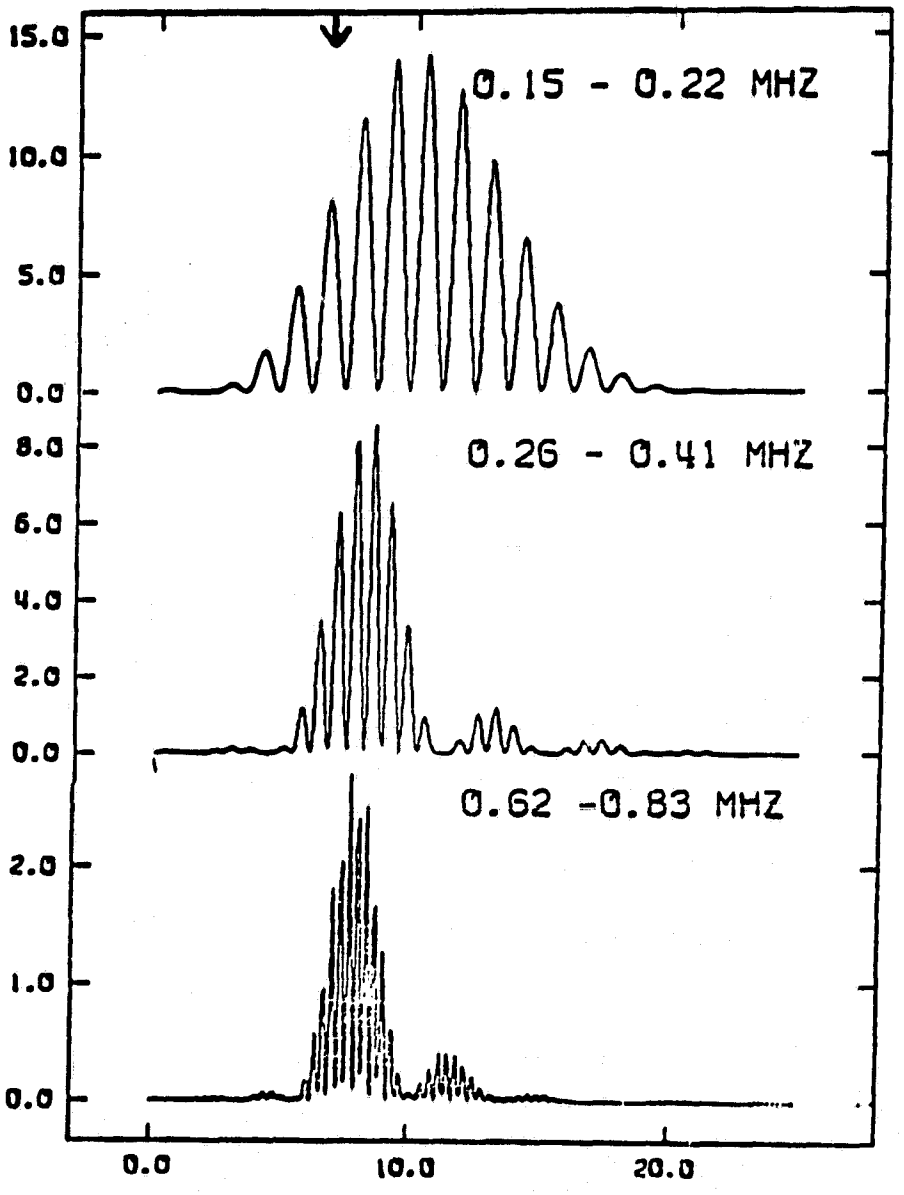

Figure 3. The Spatial Evolution of Selected Modes: Run #051606 A. Top trace: fundamental mode, $f_0 \sim 0.18$ MHz; $0.15 \leq f \leq 0.22$ MHz; Middle Trace: second harmonic, $f_2 \sim 0.34$ MHz; $0.26 \leq f \leq 0.41$ MHz. Bottom Trace: fourth harmonic, $f_4 \sim 0.72$ MHz; $0.62 \leq f \leq 0.83$ MHz. The location of the leading edge of the shock wave as seen in the raw probe is indicated by an arrow. Horizontal axis: distance (cm). Vertical axis: Amplitude squared (arbitrary units).

line-averaged techniques[10]. The analyses of fluctuations which we report avoid the bandwidth limitations of earlier reports on nonuniformities in shock waves which used hot-wire anemometry[11]. We also have shown that the recently proposed argon shock front morphology which ignores fluctuations is incomplete[12].

References

1. S.Z. Belen'kii and E.S. Fradkin, Proc.P.N. Lebedev Physics Institute 29 (1967) 197.
2. D.R. White, Phys. Fluids 4 (1961) 465.
3. J.A. Johnson III, W.R. Jones, and J. Santiago, Journal of Physics D: Applied Physics (to be published).
4. J. A. Johnson III, Appl. Phys. Letters (to be published).
5. R.E. Duff, J. Appl. Phys. 23 (1952) 1373.
6. G. Schmidt, Physics of High Temperature Plasmas, Academic Press (1979).
7. J. A. Johnson III and S.C. Chen, Phys. Letts 68A (1978) 141.
8. H.L. Swinney and J.P. Gollub, Physics Today 31 (Aug.1978) 41.
9. A.J. Raudkivi and R.A. Callander, Advanced Fluid Mechanics, Edward Arnold Press (1975).
10. I.I. Glass, W.S. Liu and F.C. Tang, Phys. Fluids 23 (1980) 224.
11. B.E.L. Deckker and M.E. Weekes, Proc. Instn. Mech. Engrs. 190 (1976) 437.
12. V. Shanmugasundaram and S.S. Murty, J. Plasma Physics 23 (1980) 43.

IV. Unsteady Turbulent Shear Flow in Shock Tube Discontinuities

In collisional fluids and plasmas, there are several mechanisms through which perturbations in unstable flow may be amplified: (1) Rayleigh-Taylor instabilities, arising when a pressure gradient is opposed by a density gradient; (2) rotational convection instabilities, arising when vortices are produced in such a manner as to enhance the spatial dimensionality of the flow; (3) ion acoustic instabilities, arising from the direct coupling of the induced electromagnetic field of the perturbation and local ion dynamics; (4) reaction-diffusion instabilities arising becasue of an inhibition of dispersion by a temporally competitive non-equilibrium process. The first two are traditional "fluid" mechansims, the second two being usually associated with with highly ionized gases. These natural instabilities can lead to turbulence in boundary layer-like flows which show two kinds of statistical fluctuations [1]: (1) random fluctuations with indeterminate phase relationships between various flow segments; (2) localized fluctuations with deterministic dynamics and fixed phase relationships from flow segment to segment. The second category (i.e., flow with "bursts" or "large coherent structures") has recently grown in importance since it plays a large role in the transport and mixing processes from which turbulence derives much of its crucial significance [2].

There is no complete theory of turbulence for these phenomena [3,4,5]. However, approaches to the problem exist which sug-

gest that (near transition) reaction rates can be distorted [6] and that a boundary layer approximation affords a generalizable quantitative context for measurements on turbulent bursts in unstable contact surfaces [7] and detonation waves [8]. Furthermore, we have just completed a study of bursting instabilities in collisional ionizing shock fronts which has analogous implications [9]. All of the results just cited have treated the instantaneous in-place manifestations of turbulence. As an extension of these interests, we report here on the real time evolution of two kinds of unstable shock tube discontinuities, both of which are boundary layerlike due either to the nature of the velocity discontinuity [10] or to the presence of curvature [11].

The flow properties of the shock tubes which we have used are summarized by the x-t plot in Figure 1. Energy is stored in a driver section: for the arc discharge tube a 14.5 μf capacitator is charged to 18.5 kV; for the pressure ruptured tube, a diaphragm contains a pressure load of between 1 to 3 atm. The energy is released by the sudden discharge ($\lesssim$20 μsec) of the capacitor in the arc-discharge shock tube and by the sudden rupturing of the diaphragm in the pressure loaded shock tube. This release causes a blast wave, or alternatively, a contact surface to propagate downstream into the driven section preceded in both cases, due to the strength of the disturbance, by a shock wave. The details concerning the production of shock waves by shock tubes are discussed in many places [12].

In the pressure ruptured tube, our measurements are performed on the contact surface. A firing to firing variation in flow velocity at the turbulent contact surface is available through the variation in primary shock wave Mach numbers, M_s, $1.5 \leq M_s \leq 3.0$ producing a range in local Reynolds number [7] of $100 \leq Re \leq 1000$. The test section contains two ports separated by 15 cm at which crossed-beam stations are placed. Blue light (4350 Å) absorption of NO_2 is used and a direct measure of the covariance of density fluctuations at the point of intersection is obtained from [13]:

$$F(x,y,z) = \frac{1}{T} \int_0^T \ln i_1(t) \cdot \ln i_2(t)\, dt = I(x,y,x)A$$

where $i_j(t)$ is the light intensity at path (j) with respect to the instantaneous average level $\langle G_j \rangle (i_j(t)/\langle G_j(t) \rangle)$, T is a convenient averaging interval, A is the cross section at the intersection of the beams, and I(x.y.z) is a measure of the intensity of turbulent density fluctuations. In the arc driven tube, our measurements are performed on the shock front. Over the length of the test section, the shock wave is heavily attenuated, providing a range of Mach numbers during a firing which can vary by as much as 5%/cm. Conventional electric probes [14] operated under ion saturation conditions are the major diagnostics. The probes are separated by 13.2 cm and give a direct measure of ion density throughout the plasma of interest. In both cases, the primary diagnostics

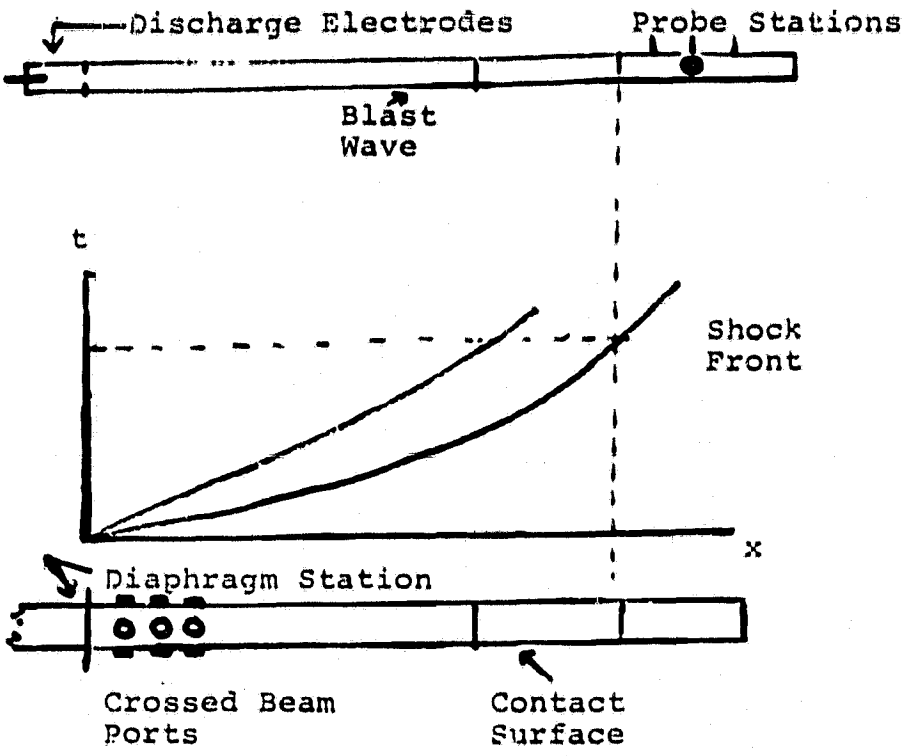

Figure 1. x-t Diagram for Shock Tube Discontinuities. The arc-discharge tube (upper sketch) is 190 cm long and 5 cm in diameter. The test section is 160 cm from the 10 cm long discharge section with inlets for electric probes as indicated above. The 12.7 cm diameter pressure ruptured shock tube (lower sketch) has a 153 cm long driver section and a 336 cm long driven section. The test section is 153 cm long, immediately adjacent to the diaphragm. See references [7], [10], and [13] for details.

are supplemented by the usual assortment of pressure gauges and line-averaged optical sensors.

First, we turn to the question of the dynamics of bursts in these two systems. Direct observations using pressure gauges roughly 3 cm apart have already provided evidence that turbulent bursts in contact surfaces propagate as discrete flow entities with velocity at roughly 90% of the local flow velocity [7]. Similarily, turbulent bursts in collisional ionizing shock fronts measured over distances of about 0.7 cm also move at velocities of roughly 90% of the local velocity; in this case, the velocity measurements are derived from the dispersion relations calculated from the power spectra [9]. These behaviors are generally consistent with the reports on large coherent structures in other manifestations of boundary layer flow [15].

A sample of the contact surface data is given in Figure 2. The driver gas is a N_2O_4 mixture {1.0%($N_2O_2 \rightleftarrows 2NO_2$); 99% He}. In Figure 2(a), the arrival of the contact surface is indicated by the sudden increase in absorption of blue light at the first and second stations. The lag in the two signals results from the time of flight between the two stations. Figure 2(a) also shows the prominent distortions in what should be otherwise a smooth monotonic change in the light signals. These are the turbulent bursts as they show up in line-averaged blue light absorption. In Figure 2(b), the covariance of each station is displayed. The signatures of the turbulent bursts

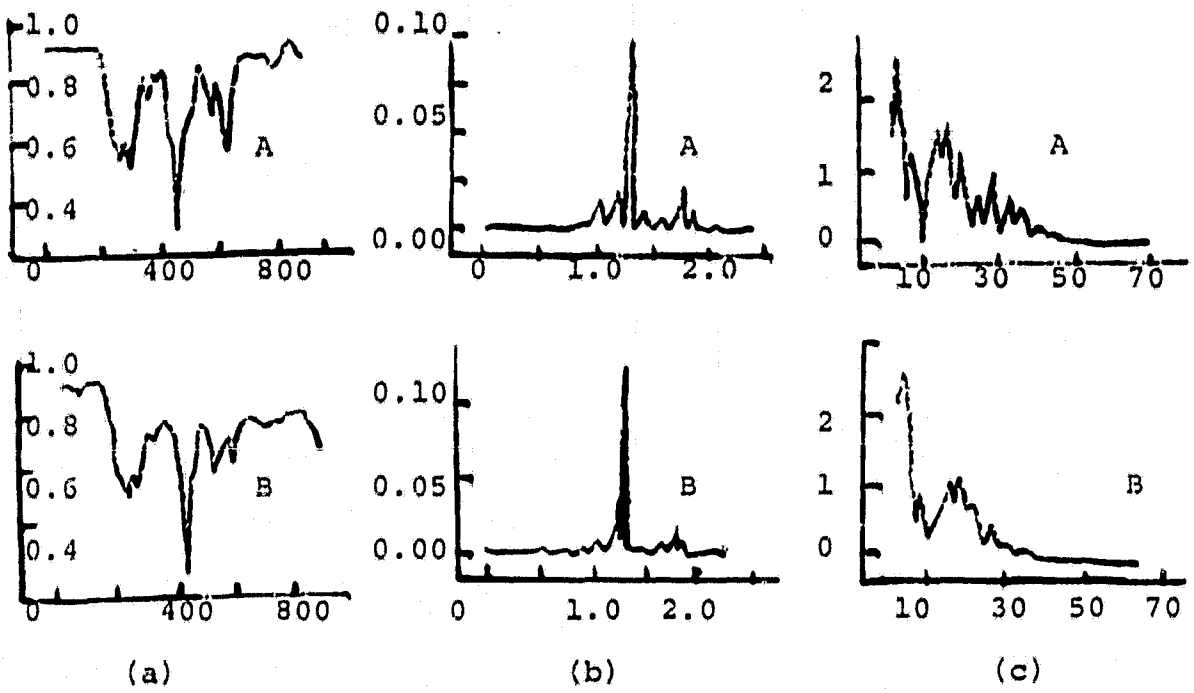

Figure 2. Crossed Beam Data: ($N_2O_4 \rightleftarrows 2NO_2$;He) Mixture for Driver Gas; N_2 for Driven Gas. (a) Light Absorption. The upper trace is the absorption in one of the two crossed beams at the first station (Station A). The lower trace is the absorption in one of the two crossed beams at the second station (Station B) 15 cm downstream. $M_{S,A} = 2.1$; $M_{S,B} = 2.3$. The vertical axes are in arbitrary (amplitude) units; the horizontal axis is sample number, 4 μs/sample. (b) Normalized Covariance I (x,y,z) for Crossed Beams. This the measure of turbulent density fluctuations, at the points of intersection, for the two stations. The vertical axes are arbitrary (power) units; the horizontal axes is local particle time in msec. (c) Power Spectra for Crossed Beams. The vertical axes are arbitrary (power) units. The horizontal axis is sample number, 122 Hz (sample).

here are the results in the region of intersection, a volume of approximately $(0.5\ cm)^3$. Power spectra for the covariance function are performed using standard FFT digital analyses and are displayed for these data in Figure 2(c). These three sets all imply a particle-like evolution of bursts. The velocity of the contact surface increases by more than 10% between stations A and B; however, the power spectra show a substantial repeating of the overall features. The results represented in Figure 2 are found in all cases studied.

A set of ion density profiles from the arc-driven shock tube is shown in Figure 3. In the top two curves, the shock front data from a single firing are given in which the argon pressure prior to discharge was 40 mTorr; the shock wave decelerates between the two stations (with 13.2 cm separation). In both cases, we can identify bursts in the plasma; we can also observe that the disturbances persist over the 13.2 cm distance. Peak to peak correspondence of the clumps can be easily traced as indicated by the assigned labels. This allows us to notice that the bursts seem to catch up with the shock fronts, a behavior of a sort consistent with a soliton-like dynamics [16]. The results represented in Figure 3 are found in all our data suggesting a particle like behavior under widely varying environments for the evolution of bursts in turbulent shock fronts.

Secondly, we have examined the evolution of the spectral behaviors of the turbulent bursts. Figure 2(c) suggests a persistance of prominent components of the spectral profile

for an accelerating discontinuity. In Figure 4, the power spectra are shown for a firing in which the contact surface decelerates by roughly 20% between the first station and the second. The gross features of the spectral profiles in terms of prominent modes are certainly reproduced in the evolution of the bursts. In firings processed to date, we find this to be the case, including the apparent tendency for a burst during its history to provide more high frequency modes, the higher its velocity.

For bursts in the shock fronts, the same general features are observed. By way of illustration, a firing is displayed in Figure 5 in which the shock front decelerates and the spectral profiles are determined. The behaviors $S_A \alpha K^{-1.39}$ and $S_B \alpha K^{-1.67}$ indicate a turbulent-like spectra dependence [17]: $S \alpha K^{\beta}$. However the differences in power law trends indicate that the relative strength of the higher wave number modes decreases as the shock front propagates and decelerates.

Finally, we turn to the possibility of an explicit connection between these bursts and other boundary layer flow. In this, we can be guided by the well established consensus with regard to the appropriateness of the treatment of contact surfaces as boundary layers [18] and in shock-tube discontinuity [8] with the Orr- Sommerfeld solutions for Falkner-Skan velocity profiles.

In the latter regard, the amplifications of fluctuations is expected to follow a predictable serpentine profile, parameterized by a characteristic frequency and a maximum in

the turbulent intensity vs Reynolds number plane [19]. This behavior is found for turbulent bursts in a boundary layer [20,18] and for turbulent bursts in a detonation wave [11,8]. Although our earlier results on contact surfaces are suggestive [7]: the pressure gauges used are wall mounted and band-width limited; the interferometer provides line-averaged (rather than point) data; and the Mach number range studied does not provide adequate determination of the change in turbulent intensity with increasing Reynolds number. However, our present data are based on point diagnostics, reach higher flow speeds with 4 times the previous bandwidth and permit us to fashion a test of the predictions of Orr-Sommerfeld-like behaviors. Specificially: (a) the strength of the fluctuations in a burst should begin to decrease with increasing Mach number $M_S \approx 2$ (see figure 12 in reference 7 and associated discussion for the relationship between shock wave Mach number and contact surface Reynolds number); (b) a single dominant frequecny should characterize the spectral profiles of fluctuations associated with the turbulent bursts.

Our data for turbulent bursts at the contact surface confirm these expectations. The local reynolds number is given by Re α ℓ where ℓ is a characteristic length scale; $\ell \alpha t_L$ where t_L is the separation between the burst and discontinuity [8]. Thus, one can map I vs t_L into I vs Re where I is the turbulent intensity. The expectation (a) above means $d^2I/dt^2_L < 0$. Figure 6(a) shows a plot of $\Delta I_x/\Delta t_L$ where, in each covariance with at least two bursts, a computation of $(I_{x,i}-I_{x,j})/$

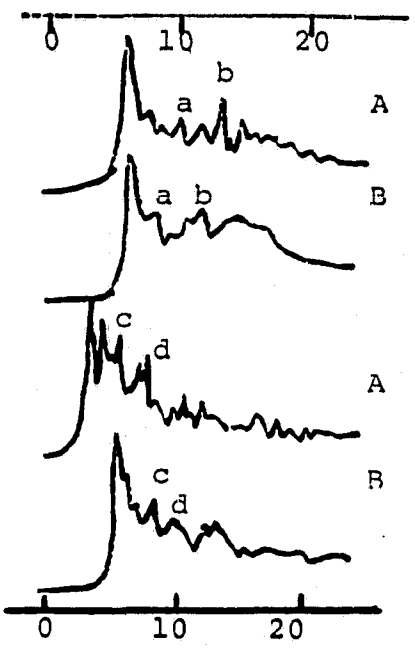

Figure 3. Electric Proble Data: Shock Heated Argon. The upper two traces give relative ion density during a discharge into Argon at initial pressure p_1=40 mTorr; $M_{S,A}$=45, $M_{S,B}$=33/ The lower traces are for p_1 = 30 mTorr; $M_{S,A}$ = 52, $M_{S,B}$=39. The vertical axes (not shown) would have been artitrary (amplitude) units; the horizontal axis in in cm; measured in a frame of reference at rest in the local gas. The labels (a,b, c,d) suggest corresponding clumps in the ion density profiles.

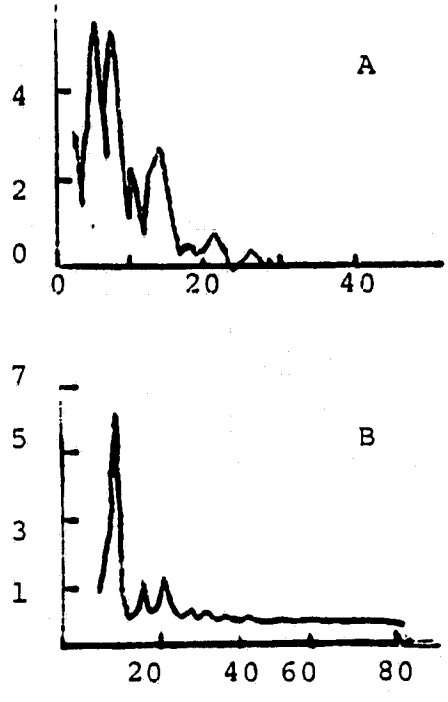

Figure 4. Crossed Beam Power Spectra: ($N_2O_4 \rightleftarrows 2NO_2;N_2$) Mixture for Driven Gas. $M_{S,A}=2.35$; $M_{S,B}=2.2$. The scales here are the same as in Figure 2(c).

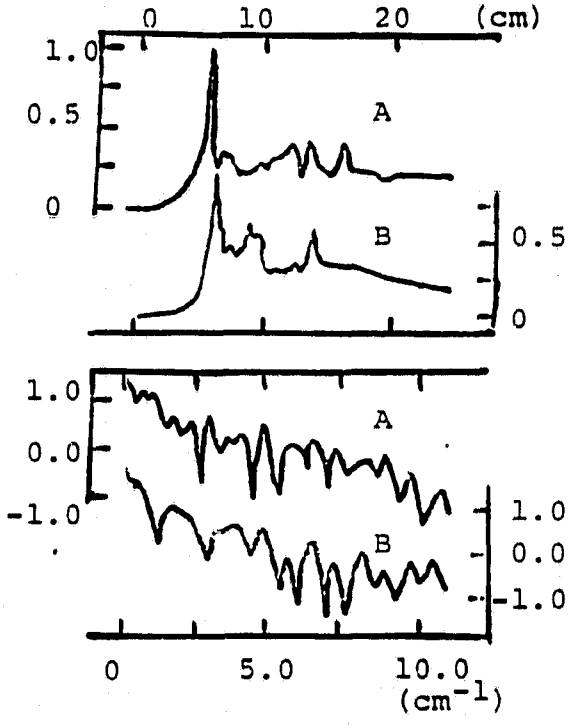

Figure 5. Ion Density Profiles and Associated Power Spectra. p_1=60 mTorr Argon; $M_{S,A}$=33, $M_{S,B}$=25. The scales for the upper two traces are the same as Figure 3. The lower two traces are the corresponding power spectra. The vertical axes are arbitrary logarithmic units; the horizontal axis is wavenumber K in cm^{-1} from $K = \omega/v_{gas}$.

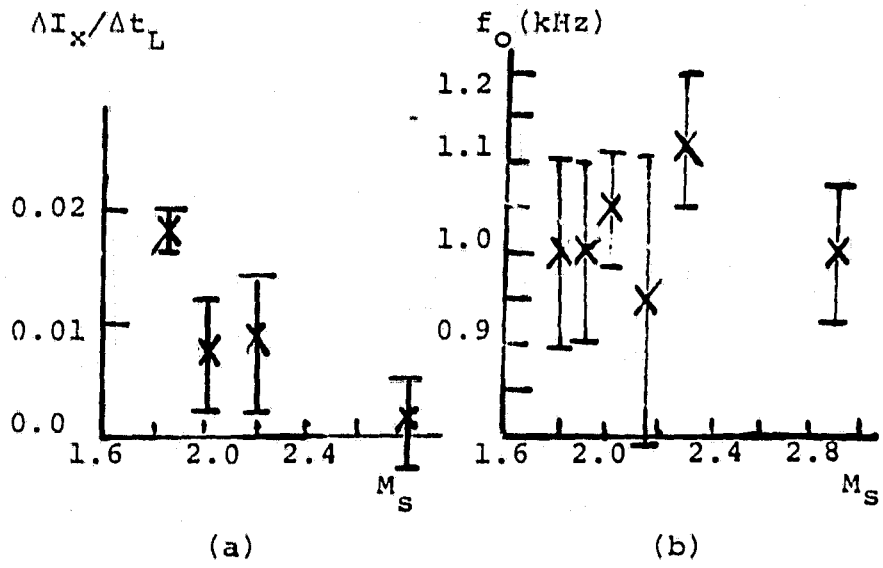

Figure 6. Crossed Beam Data on Boundary Layer-Like Profiles. (a) I_x is the value of I at the peak of an identifiable burst and t_L is the time interval between that peak and the arrival of the contact surface at the same point in a frame of reference at rest with respect to the local flow (see Figure 2). For two peaks in a given covariance profile $\Delta I_x/\Delta t_L = (I_{x,2}\ I_{x,1})/(t_{L,2}-t_{L,1})$. Each profile corresponds to a definite value for M_s. All values of $\Delta I_x/\Delta t_L$ obtained at comparable values for M_s are averaged without regard for flow history. (b) Each identifiable peak in a power spectrum, f_m, is interpreted in terms of a relationship $f_{m,i}=n_m f_i$ where $n_m=1,2,3...$ and f_i is the estimate of f_o, the fundamental frequency, provided by $f_{m,i}$. The values of f_i obtained from comparable values of M_s are averaged without regard for flow history, $f_o=\langle f_i \rangle$.

$t_{L,i}-t_{L,j}$) is performed; averages are determined at a given M_S and the profile $\Delta I_x/\Delta t_L$ vs M_S is achieved as a representation of $\Delta I/\Delta Re$ vs Re. The negative slope is qualitatively consistent with the Orr-Sommerfeld profiles. In addition, in each of the power spectra, an estimate of the fundamental mode, f_o, is made by assuming an integral relationship between it and each prominent spectral component. This given an estimate of f_o at each firing and in all spectra when we require that a single fundamental frequency should describe all data. The results are given in Figure 6(b). The average value of the fundamental frequency is $f_o \approx 1041$ Hz; the data are not inconsistent with the assumption of a constant value for this frequency over the range of speeds studies.

With these results, we see the first evidence of the possibility of nonempirical unified treatment of all boundary layer-like unsteady shear flow without regard for flow history. In particular, we see new manifestations of a "constant" characteristic frequency with these turbulent bursts of the sort previously found in conventional boundary-layer flow [21]. The usefulness of the interpretation of turbulent bursts as characterized by Orr-Sommerfeld profiles should therefore be tested for the widest possible range of flow environments.

References

1. A.S. Monin, Sov. Phys. Usp. 21, 429 (1978).

2. B.J. Cantwell, Am. Rev. Fluid Mech. 13, 457 (1981).

3. A.M. Yaglom, Am. Rev. Fluid Mech., 11, 505 (1979).

4. C. Speziale, Phys. Fluids, 23, 249 (1980).

5. M. Kac, The Boltzmann Equation (New York:Springer) 379 (1973).

6. J.A. Johnson III and S.C. Chen, Phys. Letts. 68A, 141 (1978).

7. J.A. Johnson III, W.R. Jones, and J. Santiago, J. Phys. D: Appl. Phys., 13, 1413 (1980).

8. J.A. Johnson III, Appl. Phys. Letts. 37, 275 (1980).

9. L.I., J.A. Johnson III and J.P. Santiago (submitted to Journal of Plasma Physics); also Lin I, Ph.D. dissertation 1981 (unpublished).

10. L. Landau and E. Lifshitz, Fluid Mechanics (Reading, Mass: Addison -Wesley) 114 (1959).

11. D.R. White, Phys. Fluids, 4, 465 (1961).

12. J.N. Bradley, Shock Waves in Chemistry and Physics, (London:Methuen) 88 (1962).

13. J.A. Johnson III, R. Ramaiah, and J. Santiago, Rev. Sci. Instr., (1981, to be published).

14. R.P. Smy, Adv. in Phys., 25, 517 (1976).

15. L.S.G. Kovasznay, Structure and Mechanism in Turbulence, Vol. I, H. Fiedler (ed) (New York):Springer)1(1978).

16. R.C. Davidson, Method in Nonlinear Plasma Theory, (New York:Academic), 15, (1972).

17. V.N. Tsytovich, Theory of Turbulent Plasma (New York: Academic), 15 (1972).

18. S. Tsuge, Phys. Fluids, 17, 22 (1974).

19. M.R. Osborne, SIAMJ Appl. Math 15, 539 (1967).

20. G. Schubauer and P.S. Klebanoff, NACA Report 1289 (1956).

21. R.A. Antonia, H.Q. Dank, A. Prabhu, Phys. Fluids, 19, 1680 (1976).

V. Summary

Our investigations have produced several new results. The formulation of the crossed beam correlation technique has been generalized to include strongly absorbing media. The first measurements of point density fluctuations at contact surfaces have been obtained. The presence of turbulent bursts is confirmed and a characteristic spectral frequency of approximately 400 Hz is estimated. Irregular density fluctuations with turbulent-like behaviors are found in ionizing shock fronts produced by our arc driven shock tube. We use electric probes as the primary disagnostic. Spectral analyses show statistical patterns which seem frozen-in and charactizable by a dominant mode and its harmonics. Using a pressure-ruptured shock tube and an arc driven shock tube, we have studied the evolution of turbulent fluctuations at contact surfaces with $N_2O_4 \rightleftarrows 2NO_2$ mixtures and at ionizing shock fronts in argon. We have focused on point density diagnostics derived from crossed light beam correlations and electric probes. Turbulent bursts are found for which dynamical and spectral segments with a unique and characteristic frequency, independent of flow history and overall flow conditions.

VI. Bibliography NASA Grant NSG 3280

"Turbulent Bursts in Shock Tube Discontinuities", Bull. Am. Phys. Soc. 25, 1095 (1980). (Lin I, J.A. Johnson III, and J.P. Santiago).

"Enhanced Combustion Through Turbulence", Bull. Am. Phys. Soc., 25, 1082 (1980). (J.A. Johnson III).

"Reduced Molecular Chaos and Cosmological Turbulence", Bull Am. Phys. Soc., 26, 272 (1981). (J.A. Johnson III).

"Asymtopic Behaviors for Orr-Sommerfeld Solutions", Bull. Am. Phys. Soc., 26, 444 (1981). (J.P. Santiago, J.A. Johnson III, and Y. Li).

"Density Measurements from Crossed Beams at High Extinction" Rev. Sci. Instru. (1981 , to be published). (J.A. Johnson III, R. Ramaiah, J.P. Santiago).

"Turbulence in Argon Shock Waves", Phys. Letters (1981, to be published) (J.A. Johnson III, J.P. Santiago, Lin I.)

"Unsteady Turbulent Shear Flow in Shock Tube Discontinuities," IUTAM Conference on Unsteady Turbulent Shear Flow, May 5-8, 1981; Toulose, France (1981, to be published). (J.A. Johnson III, R. Ramaiah, L.I.).

"Ionization Fluctuations in Collisional Ionizing Shock Waves", (submitted for publication). (L.I., J.A. Johnson III, J.P. Santiago).